



Cite this: *Polym. Chem.*, 2022, **13**, 2402

Reversible complexation mediated polymerization: an emerging type of organocatalytically controlled radical polymerization

Zhi-Hao Chen, Xiao-Yan Wang * and Yong Tang

As a newly developed approach of controlled radical polymerization (CRP), reversible complexation mediated polymerization (RCMP) was established in 2011 by Goto *et al.*, using iodine as a capping agent and organic molecules as catalysts (such as organic amines and organic salts), which can be regarded as an organocatalytic counterpart of ATRP. Nowadays, RCMP is attracting extensive attention, due to the constantly emerging outstanding achievements and its appealing intrinsic features including the use of inexpensive and relatively nontoxic compounds, convenient operation, various types of monomers and applicability to a range of polymer designs. Remarkably, photo-RCMP is among the most simple, inexpensive, and robust photoinduced CRPs. Their feasibility over the whole visible region and even the near-infrared region is unprecedented. In this review, we summarize in detail the research on RCMP in the last ten years since its birth, mainly focusing on the development and evolution of catalytic systems, photo-induced RCMP and the special applications derived from their inherent characteristics.

Received 27th January 2022,
Accepted 23rd March 2022

DOI: [10.1039/d2py00120a](https://doi.org/10.1039/d2py00120a)

rsc.li/polymers

1. Introduction

Controlled radical polymerization (CRP), “living” radical polymerization (LRP), or, as suggested by IUPAC, reversible-de-

activation radical polymerization (RDRP) is a rapidly developing area of chemistry and polymer science. This field has attracted much attention due to the special inherent qualities of radical polymerization, such as high functionality tolerance, high reaction rates, and importantly, the ability to precisely control the reaction process, which enable the synthesis of well-defined polymers with controlled molecular weights, functional chain ends and various topological structures. To date,

State Key Laboratory of Organometallic Chemistry, Shanghai Institute of Organic Chemistry, Chinese Academy of Sciences, 345 Lingling Lu, Shanghai 200032, China.
E-mail: wangxiaoyan@sioac.ac.cn



Zhi-Hao Chen

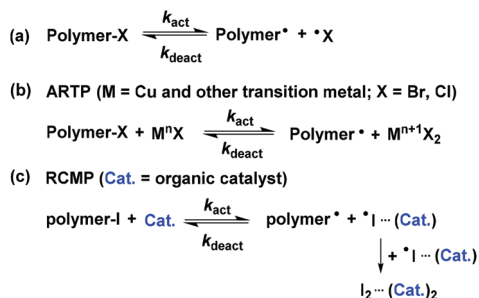
Zhi-Hao Chen received his BSc in chemistry from Qingdao University of Science and Technology in 2016, and his PhD in Organic Chemistry under the guidance of Professor Yong Tang and Associate Professor Xiaoyan Wang from Shanghai Institute of Organic Chemistry, Chinese Academy of Sciences in 2021. He is currently a postdoctoral fellow at the University of Houston. His research interest focuses on “living”/controlled free radical

polymerization and late transition metal catalyzed olefin polymerization.



Xiao-Yan Wang

Xiao-Yan Wang is currently an associate professor at Shanghai Institute of Organic Chemistry, Chinese Academy of Sciences. She graduated from Northeast Forestry University with a bachelor's degree in 2010 and received her PhD degree from Changchun Institute of Applied Chemistry, Chinese Academy of Sciences in 2015. She has mainly carried out research studies on new catalysts, controlled radical polymerization and controlled olefin coordination polymerization.



Scheme 1 The reversible activation involved in (a) general RDRP, (b) atom transfer and (c) reversible complexation.

the most popular CRP techniques include nitroxide mediated polymerization (NMP),¹ atom transfer radical polymerization (ATRP)^{2,3} or metal-mediated living polymerization, and reversible addition–fragmentation chain transfer (RAFT) polymerization.⁴ In all these procedures, control is achieved through establishing a dynamic equilibrium between the predominant dormant species and a low concentration of propagating radicals (reversible activation, Scheme 1a). There are over 2000 papers on CRP published annually, the majority of which are on transition metal mediated ATRP. This might be due to its simple experimental setup, broad range of applicable monomers and solvents, commercial availability of initiators and catalyst components, as well as exquisite control and versatility.⁵ We have recently focused on resolving the issues existing in ATRP, such as low catalyst efficiency, limited molecular weight of the polymer, as well as poor syndio-specificity and chemo-selectivity, by designing novel and efficient catalysts based on a sidearm strategy. The high stereotacticity and chemoselectivity, ultrahigh molecular weight and universality of monomers have been achieved with high efficiency, through



Yong Tang

Yong Tang is a professor at Shanghai Institute of Organic Chemistry, Chinese Academy of Sciences. He graduated from Sichuan Normal University with a bachelor's degree in 1986. He received his master's degree and doctor's degree from Shanghai Institute of Organic Chemistry, Chinese Academy of Sciences in 1992 and 1996, respectively. From 1996 to 1999, he was a postdoctoral fellow at Colorado State University and Georgetown

University. He joined Shanghai Institute of Organic Chemistry in 1999. He has been mainly engaged in research studies in organometallic chemistry, including asymmetric catalysis, olefin polymerization catalysts, ylide chemistry, total synthesis of natural products, etc.

the optimization of the catalyst structure and reaction conditions.^{6–10}

The caveat of traditional ATRP has been that the transition-metal catalysts pose challenges to the purification of polymer products and hinder their application in biomedical and electronic fields. Despite substantial strides in lowering catalyst loading and facilitating purification, organocatalysis remain highly desirable for circumventing the need for metal removal, avoiding interference with electronic systems and reducing toxicity concerns.^{11,12} In 2011, reversible complexation mediated polymerization (RCMP)¹³ was established by Goto *et al.* using iodine as a capping agent and organic molecules as catalysts (such as organic amines and organic salts), which can be regarded as an organocatalyzed counterpart of ATRP. Technically, RCMP is similar to normal ATRP (Scheme 1b) in that both include only a halogen capping dormant species and an activator (catalyst). For RCMP (Scheme 1c), amines or organic salts serve as an activator instead of Cu(I)X. More importantly, RCMP involves a reversible and relatively weak interaction between polymer-I with a catalyst (activator), leading to the generation of a polymer[•] and I-catalyst complex (deactivator). In the literature, various types of catalysts have been developed to mediate RCMP at high temperatures (40–110 °C) or under irradiation (350–780 nm) (Fig. 1). Some catalysts were only used for heat-assistant RCMP or only for photo-induced RCMP, while organic amines and pyridine *N*-oxides could mediate both types of polymerizations.

Plenty of elegant reviews that cover different aspects of ATRP have been completed by Matyjaszewski, Sawamoto and others. In contrast, to our knowledge, RCMP, as an emerging CRP strategy, has not yet been comprehensively reviewed. In 2019, Zhu and colleagues completed a review, in which the relevant studies of RCMP were briefly summarized as one of the six categories of iodine-mediated CRP.¹⁴ Meanwhile, in an excellent mini-review, Goto *et al.* summarize the recent development and applications of reversible chain transfer catalysed polymerization (RTCP) and RCMP from the perspective of halogen bonding (XB) catalysis, which refers particularly to their research studies.¹⁵ Nowadays, RCMP has attracted extensive attention due to the constantly emerging outstanding achievements and the appealing intrinsic features including the use of inexpensive and relatively nontoxic compounds, convenient operation, various types of monomers and applicability to a range of polymer designs. Therefore, a systematic and detailed review covering all the recent important progress of this field, is in high demand. Herein, we provide a comprehensive review on the research studies of RCMP in the last ten years since its birth. Firstly, the catalytic systems and their corresponding catalytic mechanisms are discussed, illustrated by heating-assistant polymerization reactions. Subsequently, photo-induced RCMP is highlighted, as photo-induced CRP is a powerful and intriguing method and has achieved significant progress in the past several decades. Finally, some special applications of RCMP derived from their inherent characteristics are briefly introduced.

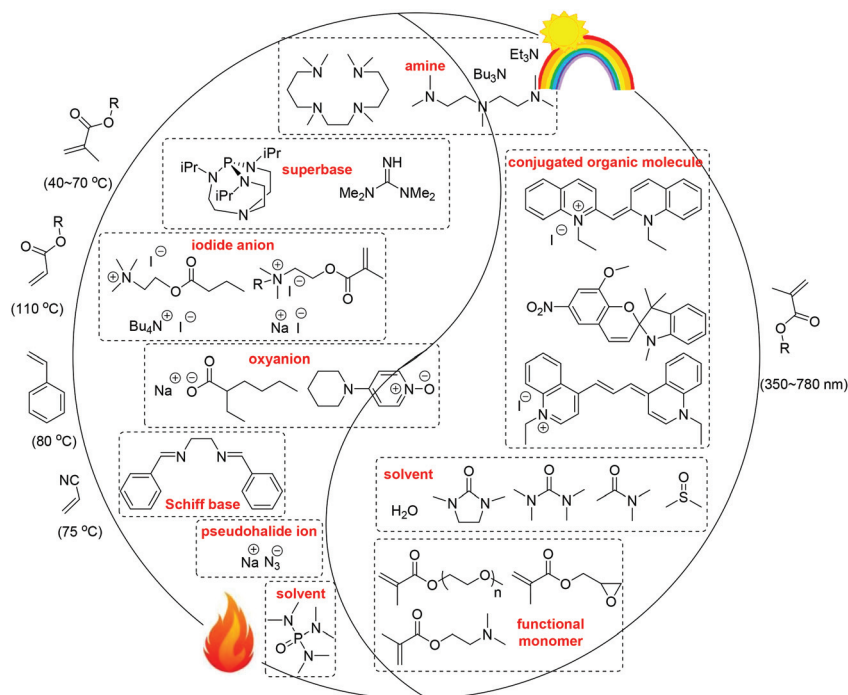


Fig. 1 The catalysts that have been reported to mediate RCMP at high temperatures or under irradiation.

2. Catalysts illustrated by heating-assistant polymerizations

The key to CRP is to maintain a low concentration of carbon-centered radicals throughout the polymerization process, based on the reversible activation of a dormant species (polymer-X) to a propagating carbon-centered radical (polymer $^{\bullet}$) (Scheme 1).^{16,17} Specific to RCMP, the control of the procedure relies on the reversible coordination between a dormant polymer-I with an organic catalyst. Therefore, catalysts are critical for RCMP, determining the controllability and efficiency of the polymerization, applicable reaction conditions (mainly including temperature and irradiation wavelength) and monomer as well as polymer properties (including end group fidelity, molecular weight and its distribution). The catalyst of RCMP should efficiently react with iodine radicals,

molecular iodine and alkyl iodide to form a complex. In order to improve the performance of catalysts and to reduce their cost and widen the application scope of RCMP, five main categories of RCMP catalysts have been developed in the last ten years (Table 1), which include organic bases (such as amines, superbases and Schiff bases), iodized organic salts (e.g., $\text{Bu}_3\text{MeP}^+\text{I}^-$ (BMPI) and $\text{Bu}_4\text{N}^+\text{I}^-$ (BNI)), alkali-metal iodides and pseudohalides (such as NaI and NaN_3), oxyanion catalysts (including pyridine *N*-oxide (PO), carboxylates, nitrates, sulfonates, and phosphates) and special solvents (e.g., hexamethylphosphoramide (HMPA)).

2.1. Organic bases

The first example of RCMP was reported in 2011 by Goto *et al.*¹³ Initially, they got an idea that even organic compounds with redox ability may work as catalysts for ATRP. To test this

Table 1 Different catalysts for heating-assistant RCMP systems

Types	Examples	Monomers and conditions	Highest M_n (kg mol^{-1}), D for PMMA	Ref.
Amine	TEA, TBA, TMTAC, PMDETA	Methacrylates (90 °C, 60 °C), styrene (120 °C), acrylonitrile (75 °C)	35.7, 1.20	13 and 18
Superbase	TiBP	Methacrylates (60 °C)	45.0, 1.45	19
Schiff base	NDBE	MMA (65 °C)	50.2, 1.39	20
Iodized organic salt	BMPI, BNI	Methacrylates (60 °C), styrene (80 °C), acrylonitrile (75 °C), BA (110 °C)	140, 1.36	21
Alkali-metal iodide and pseudohalides	NaI, KI, NaN_3	Methacrylates (40–70 °C), styrene (80 °C), acrylonitrile (75 °C), BA (110 °C)	42.0, 1.42	25 and 26
Oxyanion	PPD-PO, NaOEH	Methacrylates (50–70 °C), styrene (80 °C), acrylonitrile (75 °C)	35.0, 1.39	27 and 28
Special solvent	HMPA	MMA (60 °C)	102.3, 1.34	29

concept, they employed a well-known organic reducing agent tetra(dimethylamino)ethylene (TDAE) (Fig. 2a) as an activator catalyst instead of $\text{Cu}^{\text{I}}\text{X}$. An alkyl iodide (2-iodo-2-methylpropionitrile, CPI) was used as an initiator. It was found that in addition to TDAE, the simplest and cheapest common amines with little or a much weaker redox ability, also worked well as catalysts, such as triethylamine (TEA) and tetramethylethylenediamine (TMEDA) (Fig. 2a). They proposed a possible mechanism (Scheme 2), in which the amine abstracts an iodine from polymer-I to generate polymer $^{\bullet}$ and a complex of the iodine radical with the amine (I^{\bullet} /amine complex). The unstable iodine radical recombines with another iodine radical to form a complex of the iodine molecule and amine (I_2 /amine complex). Polymer $^{\bullet}$ reacts with these complexes (deactivators) to form polymer-I and the amine.

The bulk polymerization of MMA (100 equiv.) at 90 °C with TEA (0.5 equiv.) as an activator catalyst and CPI (1 equiv.) as an initiator gave a 66% monomer conversion in 2.3 h. No polymerization proceeded in the absence of CPI or TEA, confirming that the radical was generated by the combination of TEA and CPI. However, the polydispersity index ($D = M_w/M_n$) was larger than 1.5 and M_n deviated from the theoretical value $M_{n,\text{theo}}$ at an early stage of polymerization. This indicates that many monomers added to polymer $^{\bullet}$ at the initial stage of polymerization due to insufficient deactivators (I_2 /amine complex) being accumulated. In the presence of a small amount of I_2 (as small as 1/40 equiv. to catalyst), M_n agreed with $M_{n,\text{theo}}$ and D remained small (about 1.2) from an early stage of polymerization up to high conversions. D became

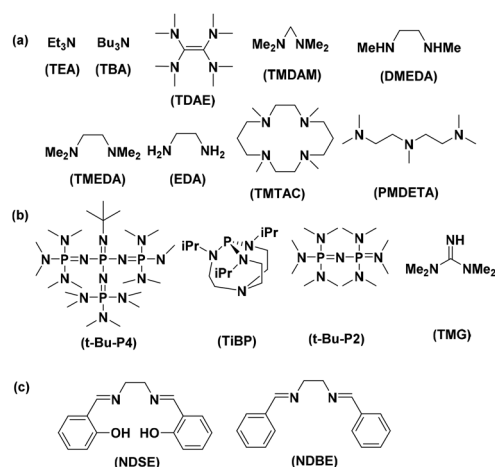
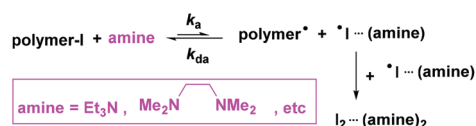


Fig. 2 Structures of (a) amine catalysts, (b) superbases and (c) Schiff base catalysts.



Scheme 2 Reversible activation in RCMP catalyzed by organic amines.

larger in the order of tertiary amine TMEDA < secondary amine dimethylethylenediamine (DMEDA) < primary amine ethylenediamine (EDA), demonstrating that the number of alkyl groups attached to nitrogen was important. Thus, tertiary amines are the most effective, due to a higher electron density on the nitrogen with a greater number of alkyl groups and hence a higher coordination ability. As a primary amine, EDA causes a particularly significant side reaction, *i.e.*, a chain-end transformation of polymer-I (dormant species) to polymer-NH-R (inactive species). This side reaction is much faster for primary amines, compared with secondary and tertiary amines. The homopolymerizations of some other monomers such as styrene (St), acrylonitrile (AN), and functional methacrylates with a hydroxyl group (HEMA) and a benzyl group (BzMA) afforded polymers with a relatively low polydispersity ($D = 1.28\text{--}1.49$) even at high conversions (>70%). All of these polymerizations are heating-assisted bulk polymerizations. Notably, for AN, methacrylates and styrene, the reaction temperatures are 75 °C, 90 °C and 120 °C, respectively, based on the strength of the carbon–iodine bond at the polymer chain end.

RCMP relies on reversible complexation, which is a new reversible activation mechanism of CRP and was supported by three experiments. (a) The tacticity of the polymer obtained is virtually the same as that for a conventional free radical polymerization and the present polymerization was also completely inhibited in the presence of a radical scavenger, demonstrating that the propagating species is a free radical. (b) In a model experiment of CPI and TEA at 70 °C, the characteristic UV absorptions of the I_2 /TEA complex at 360 and 302 nm were observed after 2 h, confirming the formation of the I_2 /amine complex. (c) The model experiment of the I_2 /TEA complex and an azo compound (V601) produces the adduct of the unimer radical and iodine (MMA-I), demonstrating the role of the I_2 /amine complex as a deactivator. For the PMMA-I/TMEDA system, the k_{a} ($0.13 \text{ M}^{-1} \text{ s}^{-1}$) was large enough but the k_{da} ($7.2 \times 10^5 \text{ M}^{-1} \text{ s}^{-1}$) was relatively small, which explain why the system yields low-polydispersity polymers from an early stage of polymerization and the system requires the addition of a small amount of deactivator at the beginning of polymerization.

In 2016, Bai and co-workers¹⁸ employed pentamethyldiethylenetriamine (PMDETA) as an efficient catalyst for bulk RCMP using CPI as the initiator, giving an MMA conversion of 84.5% after 16 h. Compared with TEA and TMEDA employed by Goto's group, PMDETA achieved relatively faster polymerization rates and relatively lower M_w/M_n values of the obtained polymers under the same conditions. In the presence of alkyl iodides, Goto and co-workers¹⁹ demonstrated the application of superbases as highly active catalysts in RCMP, including a guanidine (TMG), an aminophosphine (TiBP) and phosphazenes ($t\text{-Bu-P}_4$ and $t\text{-Bu-P}_2$) (Fig. 2b). At mild temperatures (60–80 °C), these catalysts enabled the synthesis of low-polydispersity polymers through high conversions (*e.g.*, 80%) in reasonably short times (*e.g.*, 3–12 h) for MMA, St and three functional methacrylates. In 2019, Shi's group reported that Schiff bases, including N,N -dibenzylidene-1,2-diaminoethane

(NDBE) and *N,N'*-disalicylidene-1,2-diaminoethane (NDSE), were efficient organic catalysts for the RCMP of MMA (Fig. 2c), affording well-defined and low-polydispersity polymers ($M_w/M_n = 1.2\text{--}1.4$) at mild temperatures (65–80 °C).²⁰

2.2. Iodized organic salts

Generally, RCMP catalyzed by organic amines has important limitations, particularly with respect to molecular weight and monomer versatility. The monomer scope was limited to methacrylates and styrenics, and the controlled polymerization of acrylates was challenging. The molecular weight was limited to approximately 10 000 in most cases. To address these challenges, more reactive catalysts were developed by Goto *et al.*, which were common and inexpensive organic salts such as tetrabutylammonium iodide ($\text{Bu}_4\text{N}^+\text{I}^-$ (BNI)), methyltributylphosphonium iodide ($\text{Bu}_3\text{MeP}^+\text{I}^-$ (BMPI)), and ethylmethylimidazolium iodide (EMZI) (Fig. 3a).²¹ They heated a mixture of MMA (8 M) with CPI (80 mM) under the catalysis of BNI or BMPI (40 mM) at 70 °C, achieving over 80% monomer conversion in very short times (3–4 h).

Notably, the catalysts enabled controlled polymerization of acrylates and the synthesis of high molecular-weight polymers (up to $M_n = 140\,000$). Higher molecular weights are important for tuning mechanical, thermodynamic, and optical properties in materials design. BMPI was chosen as a catalyst to maintain a sufficiently large R_p , employing a mild temperature of 40–60 °C for the synthesis of high-molecular-weight PMMA to suppress the elimination of HI side reaction. The addition of an amine or a small amount of an azo compound helps overcome the rather slow polymerization because of the low concentration of CPI. An amine traps the radical polymerization inhibitor HI and also functions as an additional activator. R_p is increased by using an azo compound to supply polymer \cdot . On the other hand, the carbon–iodine bond in an acrylate polymer (with a secondary alkyl chain end) is stronger than that in a methacrylate polymer (with a tertiary one). Therefore, BMPI and BNI with high reactivity were used as the catalysts for controlling acrylate (butyl acrylate, BA) polymerization at a higher temperature of 110 °C, which yielded polymers with low-polydispersity ($D = 1.2\text{--}1.4$) for both catalysts. However, the polymerization rate was much slower compared with that of MMA polymerization. Besides, the use of alkyl iodide formed *in situ* (the I_2 /azo method) was effective for higher targeted DPs by BMPI and BNI. Elemental and NMR analyses demon-

strated the high fraction of iodine chain ends in the polymers obtained with BMPI at 60 °C (92%–99%). Methacrylate and acrylate block copolymers were also synthesized without being confined to the monomer order of addition.

The authors propose the reversible activation mechanism for organic salt catalysts. An iodide anion (A^+I^-) activates polymer-I, producing polymer \cdot and an I_2 radical anion ($\text{A}^+\text{I}_2^{\cdot-}$) (Scheme 3a). The $\text{A}^+\text{I}_2^{\cdot-}$ radical is unstable, and thus two $\text{A}^+\text{I}_2^{\cdot-}$ species react with each other to produce A^+I^- and a stable I_3^- anion (A^+I_3^-) (Scheme 3b), which behave as an activator and a deactivator, respectively. Polymer \cdot can thus be deactivated by either $\text{A}^+\text{I}_2^{\cdot-}$ or A^+I_3^- (Scheme 3c). The formation of A^+I_3^- was probed by UV–vis absorption during the polymerization of MMA with BNI and CP-I at 80 °C. They demonstrated that A^+I_3^- acts as a deactivator by the model experiment of Bu_4NI_3 and an azo radical source V601 that produces a model unimer radical of MMA at 60 °C, in which the adduct of the unimer radical and iodine (MMA-I) was observed. The gel permeation chromatography (GPC) peak resolution method was utilized and the k_a values for BMPI and BNI were found to be $0.30\text{ M}^{-1}\text{ s}^{-1}$ and $0.43\text{ M}^{-1}\text{ s}^{-1}$, respectively. These values are larger than the k_a value ($0.13\text{ M}^{-1}\text{ s}^{-1}$) for TMEDA,²² which is a representative good amine catalyst.

Inspired by the biocompatibility and metabolizability of choline and its analogues, Goto's group used nontoxic catalysts for the RCMP of several methacrylates and acrylates, including choline iodide (ChI), acetylcholine iodide (AChI) and butyrylcholine iodide (BChI) (Fig. 3b).²³ This is an alternative approach to the ppm-level copper catalyst and iron-based catalytic systems in sustainability aspects in green polymer chemistry. An appropriate amount of NaI is also nontoxic. CPI was replaced with α -iodophenylacetate (EPHI) and ethyl 2-iodo-2-methylpropionate (EMAI) as alkyl iodide initiators, so that the synthesized polymers did not bear the toxic nitrile moiety. In all cases, the polymerization was conducted in bulk or in a biodegradable and nontoxic green solvent (ethyl lactate (EL), ethanol, or water). Therefore, all polymerizations are green systems.

The bulk polymerization of MMA (8 M) with EPHI (80 mM) and BChI (80 mM) at 70 °C afforded a 73% monomer conversion in 10 h. The polydispersity index was approximately 1.2 from an early stage of polymerization, and the number-average molecular weight (M_n) agreed with the theoretical value. In the presence of EMAI (80 mM) and BChI (320 mM), a 48% monomer conversion in 48 h was achieved in the solution polymerization of BA (8 M) in 25 wt% EL at 110 °C. The low-polydispersity of the resultant polymers demonstrated the high activity of BChI.

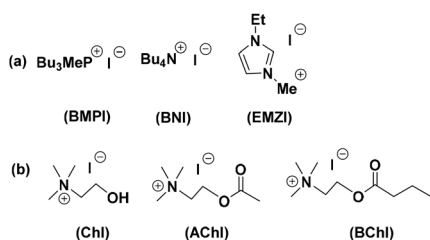
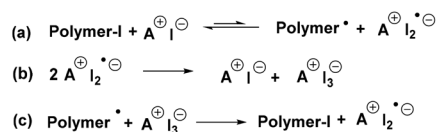


Fig. 3 (a) Structures of organic salt catalysts and (b) structures of organic salt catalysts in green RCMP systems.



Scheme 3 Possible mechanism of reversible activation with an organic salt catalyst.

Taking advantage of the high solubility in polar media and high catalytic activity, choline iodide catalysts were also successfully utilized in the polymerizations of poly(ethylene glycol) methyl ether methacrylate (PEGMA) and 2-hydroxyethyl methacrylate (HEMA) for possible biomedical applications. A relatively low temperature (55 °C or below) was set for these methacrylates to suppress the significant elimination of HI from the polymer chain end in polar media. The polymerization rate (R_p) was improved by adding an azo initiator, 2,2'-azobis(2,4-dimethyl-valeronitrile) (V65) to decrease the deactivator concentration. In addition to the functional methacrylates, functional acrylates were also successfully used, including poly(ethylene glycol) methyl ether acrylate (PEGA) and 2-methoxyethyl acrylate (MEA). The polymerizations of zwitterionic sulfobetaine methacrylate (SBMA) and 2-methacryloyloxyethyl phosphorylcholine (MPC) were also successfully conducted. This is the first controlled synthesis of zwitterionic polymers *via* the organocatalytic CRP. Well-defined amphiphilic block copolymers were also synthesized. The attractive features of this polymerization system include accessibility to a range of polymer designs and the use of nontoxic choline iodide catalysts as well as green polymerization conditions, which can contribute to sustainable polymer chemistry.

Subsequently, they reported the self-catalyzed controlled radical polymerization using quaternary ammonium iodide (QAI)-containing monomers.²⁴ The monomer contains a polymerizable acrylate or methacrylate moiety and QAI as a catalytic moiety at the side chain. They firstly carried out self-catalyzed RCMPs of MMA as a main monomer and C₆MAI as a catalytic comonomer at 70 °C by varying the ratios of [MMA]₀/[C₆MAI]₀ from 99/1 to 75/25 using CPI as the initiator. The solvent ethylene carbonate (EC) was used to dissolve C₆MAI for high C₆MAI-content systems ([MMA]₀/[C₆MAI]₀ = 90/10 and 75/25). The monomer consumption rate was very similar for MMA and C₆MAI, indicating that the reactivity ratios are nearly 1. A total monomer conversion of 69% was obtained for 4 h. The dispersity was low (1.17–1.34) and the M_n was close to the theoretical value. The polymer composition (MMA/C₆MAI) matched the feed monomer composition, indicating the nearly unity reactivity ratio. By increasing the C₆MAI fraction, the polymerization rate reasonably enhanced due to the higher catalyst (C₆MAI) concentration.

All the MMA polymerizations were effective with catalytic monomers (CMs) possessing different alkyl chains (Fig. 4), *i.e.*, butyl (C₄MAI), octyl (C₈MAI), 2-ethylhexyl (EHMAI), dodecyl (C₁₂MAI), and allyl (AMAI) chains, giving polymers with low-dispersity (\bar{D} = approximately 1.3). Besides, various QAI-containing copolymers with low-dispersity ($\bar{D} \leq 1.40$) were success-

fully synthesized, demonstrating that the QAI-containing monomers were compatible with various functional methacrylates and acrylates. Self-catalyzed block polymerizations were achieved without additional catalysts, employing the obtained QAI-containing polymers as catalytic macroinitiators. The self-catalyzed RCMP also enabled the synthesis of a QAI-containing polymer brush. The beneficial aspects include the high versatility in amenable monomers and CMs and the metal-free nature, and the obtained polymers may find antibacterial and biomedical applications.

2.3. Alkali-metal iodides and pseudohalides

In the aforementioned studies, Goto *et al.* utilized iodide anions (I⁻) as highly reactive catalysts for RCMP, which contain organic counter cations, such as Bu₃MeP⁺I⁻ and Bu₄N⁺I⁻, based on which they further pursued the use of alkali metal and alkaline earth metal cations as counter cations (A⁺).²⁵ The bulk polymerizations of MMA (8 M, 100 equiv.) were conducted at 70 °C, using CPI (80 mM, 1 equiv.) as the initiator. The catalysts they studied included alkali metal iodides (40 mM, 0.5 equiv.), NaI, KI, and CsI and alkaline earth metal iodides MgI₂ and CaI₂. 18-crown-6-ether (40 mM, same equivalent as the catalyst) was employed to solvate the catalysts. NaI achieved the best result, in which the relatively high polymerization rate R_p (conversion = 83% in 4 h) is attractive. The \bar{D} was approximately 1.2 from the early stage of polymerization, and the M_n matched well with the theoretical value. No polymerization occurred without a catalyst, suggesting that the radical was generated due to the reaction of CPI with the catalyst. KI was also efficient as a catalyst for achieving low \bar{D} and controlling M_n , although affording a slightly slower polymerization than NaI. CsI resulted in a much slower polymerization. In addition to the solubility issue, the counteraction may affect the catalytic activity *via* the associated and dissociated equilibrium. MgI₂ and CaI₂ were ineffective as catalysts, as they were virtually insoluble in MMA with 18-crown-6-ether. Moreover, I₂²⁻ is the anion for MgI₂ and CaI₂ and might not facilitate efficient catalysis compared with I⁻. The NMR analysis of the polymer obtained with the NaI catalyst suggested that the fraction of the iodine chain end was ~100% (with ±8% experimental error).

Compared with 18-crown-6-ether, diglyme is environmentally friendly and more inexpensive, and was also studied as the solvent. NaI was completely dissolved in the polymerization system, resulting in a small \bar{D} value (1.2–1.3). However, the other four catalysts yielded much smaller R_p values, as they were not well dissolved with diglyme. These results suggest the high efficiency of NaI compared with the other four studied catalysts. Diglyme led to slower polymerization than 18-crown-6-ether, and this shortcoming could be overcome by adding a small amount of an azo initiator V65. The polymerization also proceeded smoothly after the induction period of ~2.5 h, by using alkyl iodide formed *via in situ* reaction of an azo compound with I₂. The conversion reached 98% in 6 h with a narrow \bar{D} (approximately 1.2), and the M_n agreed well with $M_{n,theo}$. Using an isolated alkyl iodide CPI or using the I₂/azo

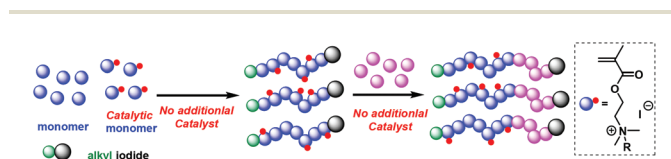
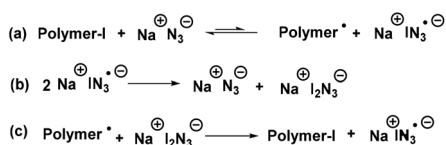


Fig. 4 The self-catalyzed controlled radical polymerization.

method, they also carried out the polymerizations of St, AN, and functional methacrylates with benzyl (BzMA), lauryl (LMA), hydroxyl (HEMA), dimethylamino (DMAEMA), and polyethylene glycol (PEGMA) groups. The polymerization was regulated with high conversions ($\geq 75\%$) in all studied cases. Besides, the accessibility of the NaI system was illustrated by a wide range of polymer architectural designs (chain-end functional, diblock, triblock, and star polymers).

Goto *et al.* further investigated pseudohalides such as an azide anions (N_3^-) as catalysts for RCMP.²⁶ They conducted the RCMP of MMA by heating a mixture of MMA (8 M), CPI (80 mM), and NaN_3 (40 mM) as a catalyst at 70 °C, using 18-crown-6 ether (40 mM) to solvate NaN_3 . The polymerization yielded a monomer conversion of 80% in 5 h; however, the D was larger than 1.5 at the beginning of polymerization. The addition of a small amount of I_2 resulted in small D (approximately 1.2) and high conversions ($\sim 90\%$), thereby demonstrating the success of this CRP. They proposed the following mechanism. Polymer-I is activated by Na^+N_3^- , generating polymer \cdot and $\text{Na}^+(\text{IN}_3^{\cdot-})$. Many monomers are added to polymer \cdot before polymer \cdot is deactivated to regenerate polymer-I (Scheme 4a). Because $\text{Na}^+(\text{IN}_3^{\cdot-})$ is not stable, two $\text{Na}^+(\text{IN}_3^{\cdot-})$ species may react with each other to produce stable species Na^+N_3^- and $\text{Na}^+(\text{I}_2\text{N}_3^-)$ (Scheme 4b). Na^+N_3^- acts as an activator, while $\text{Na}^+(\text{I}_2\text{N}_3^-)$ works as a deactivator (Scheme 4c). Polymer \cdot can thus be deactivated by either $\text{Na}^+(\text{IN}_3^{\cdot-})$ or $\text{Na}^+(\text{I}_2\text{N}_3^-)$. ^-OCN (NaOCN) and ^-SCN (NaSCN, $\text{Bu}_4\text{N}^+(\text{SCN}^-)$) are also used as catalysts. In all cases, the polymerization proceeded smoothly, M_n well matched $M_{n,\text{theo}}$, and D was small (approximately 1.2). Thus, N_3^- , ^-SCN , and ^-OCN all worked as efficient catalysts of CRP. The monomer scope of the NaN_3 catalyst included other hydrophobic methacrylates with benzyl (BzMA), butyl (BMA), and lauryl (LMA) groups as well as MMA. In a hydrophobic solvent (50% toluene), the methacrylate with a PEGMA group was also successfully used. Besides methacrylates, the NaN_3 , BNSCN, and NaOCN catalysts were efficient for an acrylate, butyl acrylate (BA), resulting in low polydispersity ($D = 1.2\text{--}1.3$), although with relatively slow polymerization.

More intriguingly, the one-pot synthesis of N_3 -chain-end-functionalized polymers was achieved with the dual use of N_3^- for catalysing the CRP in “nonpolar” solvents and the following chain-end transformation in “polar” solvents (substitution agent) by the addition of polar solvents after the CRP (Fig. 5). PMMA-I was obtained by heating a mixture of CPI (270 mM), NaN_3 (300 mM), MMA (8 M), I_2 (3 mM), 18-crown-6 ether (300 mM), and toluene (toluene/MMA = 25/75%) at 70 °C for 3 h. By directly adding the polar solvent *N,N*-dimethyl-



Scheme 4 Possible mechanism of reversible activation with an N_3^- catalyst.



Fig. 5 One-pot synthesis of an N_3 -chain-end-functionalized polymer via solvent-dependent dual works of NaN_3 .

formamide (DMF) (DMF/polymerization solution = 2/1) to the polymerization solution, PMMA- N_3 was obtained after 12 h at room temperature without significant changes of M_n ($= 3400$) and D ($= 1.16$). The polymer after the transformation was studied by elemental analysis, which suggests that the fraction of N_3 at the chain end was $\sim 90\%$ (with 10% experimental error), confirming a high yield of PMMA- N_3 . Notably, this approach enabled the preparation of N_3 -chain-end polymethacrylates without utilizing a large excess of azide.

2.4. Oxyanion catalysts

Among the aforementioned catalysts, the ionic catalysts (I^- and N_3^-) showed much higher catalytic activities than the neutral amines due to their higher electron-donating ability. However, because of no substituent on these anions, it is impossible to manipulate their catalytic activities sterically or electronically. Based on this background, Goto *et al.* employed ionic pyridine *N*-oxide ($\text{C}_5\text{H}_5\text{N}^+\text{O}^-$) (PO) and its substituted derivatives as catalysts (Fig. 6).²⁷ The O^- moiety of PO catalysts can coordinate iodide, and the catalytic activity can be tuned by varying the substituents of PO. This is an attractive feature of PO catalysts over the previous ionic catalysts. Besides, the good solubility in nonpolar monomers makes PO catalysts more favourable in practical applications.

For *para*-substituted POs, the monomer conversion increased following the order of nitro (0%) \sim hydrogen (0%) $<$ phenyl (14%) $<$ methyl (27%) $<$ methoxy (42%) $<$ dimethylamino (69%) substituents, suggesting a clear trend that a stronger electron-donating substituent brought a higher catalytic activity. This is because the increased electron density on the O^- moiety enhanced halogen bonding. With methoxy, phenyl, methyl, and dimethylamino-substituted POs, the M_n value well matched the theoretical value, and the D value was

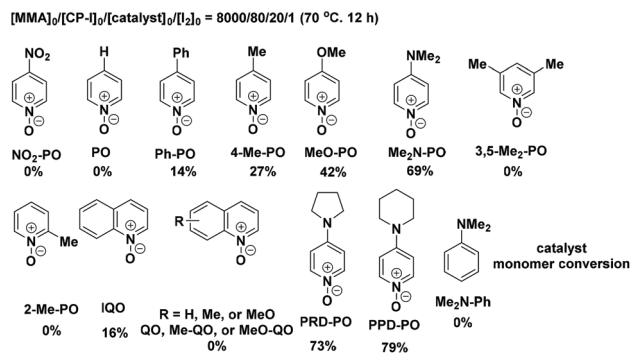


Fig. 6 Structures and abbreviations of the studied PO catalysts and results of MMA polymerizations.

low (1.15–1.25), demonstrating a highly controlled polymerization. For the methyl substituent, the *para*-substituted PO (4-Me-PO) gave 27% monomer conversion; however, no polymerization occurred with the *meta*- and *ortho*-substituted POs (3,5-Me₂-PO and 2-Me-PO). This is because the *ortho*-substitution gives steric hindrance at the O[−] moiety and the *meta*-orientation is less effective to increase the electron density of the O[−] moiety. Quinoline oxides with extended aromaticity (IQO, QO, Me-QO, and MeO-QO) resulted in lower catalytic activities than POs because of the electron delocalization (lower electron density on the O[−] moiety). Two cyclic dialkylamino-POs, *i.e.*, 4-(piperidin-1-yl)pyridine *N*-oxide (PPD-PO) and 4-(pyrrolidin-1-yl)pyridine *N*-oxide (PRD-PO), afforded similar monomer conversions of 73–79% in 12 h. In all cases, the M_n values were close to the theoretical values with small D values (~ 1.2) from the initial stage of polymerization, indicating a sufficiently fast activation process.

While PPD-PO was effective as a catalyst, the R_p was relatively low (79% conversion after a relatively long time of 12 h). The addition of a small amount of an azo initiator (V65) effectively overcame the slow polymerization, which is often employed in other controlled radical polymerizations. Besides, the polymerization by the PPD-PO catalyst was amenable to a variety of hydrophilic and hydrophobic methacrylates with (dimethylamino)ethyl (DMAEMA), poly(ethylene glycol) (PEGMA), 2-hydroxyethyl (HEMA), benzyl (BzMA), butyl (BMA), lauryl (LMA), and 2,2,2-trifluoroethyl (TFEMA) groups. In all cases, low-dispersity ($D = 1.14$ – 1.49) polymers were obtained with high conversions (70–95%).

The use of oxygen-centered anions (O[−]) opened a new avenue in catalyst development in RCMP, as the pyridine *N*-oxide derivatives worked as efficient catalysts. However, the practical applications were limited, due to their rigid aromatic structure and multi-step synthesis. Very recently, carboxylates, nitrates, sulfonates, and a phosphate (Fig. 7) were utilized as RCMP oxyanion catalysts combined with CPI. Unlike pyridine *N*-oxide derivatives, these oxyanion families enable various molecular designs because of their simple structures and abundance in natural, biological, and synthetic chemistries.²⁸

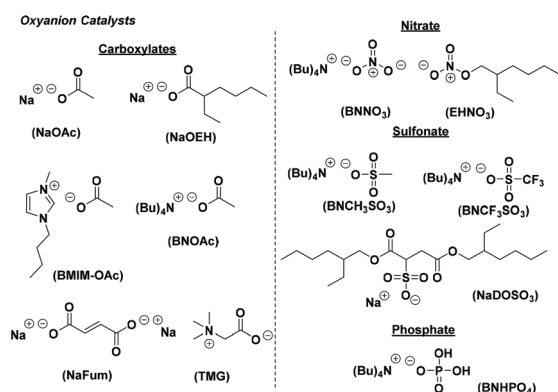


Fig. 7 Structures of the oxyanion catalysts.

The polymerization of MMA was carried out at 70 °C, using CPI (80 mM) as an alkyl iodide initiator, sodium acetate (NaOAc) (80 mM) as a catalyst, and 18-crown-6-ether (80 mM) to dissolve the catalyst. After an induction period of 4 h due to a slow dissolution of NaOAc, the polymerization proceeded smoothly achieving monomer conversions up to 80% in 10 h and a narrow D value below 1.2. No polymerization occurred in the absence of NaOAc or 18-crown-6-ether, suggesting that the NaOAc dissolved by the crown ether worked as a catalyst. Generally, a higher basicity (a higher nucleophilicity) is beneficial for promoting halogen bonding catalysis due to the stronger halogen bonding. However, too high basicity results in significant elimination as a competitive side reaction. NaOEH brought no induction period due to the good solubility and hence led to faster polymerization, achieving 75% monomer conversion in 3 h. However, NaOEH is a highly active catalyst to rapidly generate a large amount of alkyl radicals from alkyl iodides, which led to significant termination among short oligomer radicals and an M_n value deviating from the $M_{n,theo}$ value. With the addition of I₂ (5 mM), the M_n value matched well the $M_{n,theo}$ value and the D value was small (below 1.2) from the initial stage of polymerization. Using metal-free catalysts, tetrabutylammonium acetate (BNOAc) and 1-butyl-3-methylimidazolium acetate (BMIM-OAc), polymers with D values of 1.24–1.30 were obtained. However, even in the presence of I₂ (deactivator), the M_n value deviated from the $M_{n,theo}$ value for both catalysts, probably because of the HI elimination. Similar to tetrabutylammonium nitrate (BNNO₃), tetrabutylammonium methanesulfonate (BNCH₃SO₃) was effective as a catalyst and achieved good agreement of M_n with $M_{n,theo}$ and low D values (≤ 1.28), indicating a minor occurrence of the elimination. Different from the successful polymerization with methyl sulfonate (BNCH₃SO₃), no polymerization took place with trifluoromethanesulfonate (tetrabutylammonium trifluoromethanesulfonate (BNCF₃SO₃)). This might be due to the electron-withdrawing trifluoromethyl group reducing the basicity (nucleophilicity) of SO₃[−] and suppressing the halogen bonding catalysis. The basicity of PO₄[−] is relatively high, and thus the polymerization with tetrabutylammonium phosphate monobasic (BNHPO₄) resulted in a marked deviation of M_n from $M_{n,theo}$ attributed to the elimination of HI. Among the studied oxyanions, BNNO₃ and NaOEH are particularly useful catalysts with respect to their high polymerization rates and good controllability. Naturally existing oxyanions, including trimethylglycine (TMG), sodium fumarate (NaFum) and sodium dioctyl sulfosuccinate (NaDOSO₃) were also successfully employed as catalysts for the polymerization of MMA with a small amount of V65 (10 mM). Besides, these oxyanion catalysts were amenable for functional methacrylates, acrylonitrile, and styrene, and also yielded block copolymers with low D values.

2.5. Solvent

As a cheap and easy-to-handle phosphoramidate, hexamethylphosphoramide (HMPA) is a highly polar, aprotic solvent with widespread use in organic synthesis as a solvent or an additive

and can form a complex with both alkyl halide and iodine molecules. In 2017, Shi *et al.* used HMPA as a highly efficient organic catalyst for the controlled polymerization of MMA, employing 2,2-azobis(isoheptonitrile) (ABVN) and I_2 as starting compounds to form alkyl iodide *in situ*. The bulk polymerizations of MMA were rapid without an inhibition period and demonstrated typical features of CRP.²⁹ It is obvious that the solution polymerization under similar conditions can be divided into an inhibition period and a polymerization period. Notably, the induction period was shortened as the dosage of the catalyst increased, suggesting that the decomposition rate of ABVN was enhanced by HMPA. Moreover, the polymerization rate was higher on increasing the amount of HMPA, and the M_w/M_n values of the polymers produced with HMPA were much lower (<1.22) than those of polymers without HMPA (>1.5), suggesting a higher polymerization rate and a faster activation–deactivation cycle induced by HMPA. Notably, high-molecular-weight polymers with a narrow molecular weight distribution were successfully produced (M_n up to 104 000, $M_w/M_n = 1.34$). The chain extension and block copolymerization confirmed the living feature of the obtained polymers. In order to achieve a high polymerization rate, the RCMP catalysed by HMPA in this study requires a continuous supply of new initiating radicals to consume the deactivators.

3. Photo-induced/controlled RCMP

Photoinduced reactions are widely used in organic synthesis and polymer synthesis. The reactions do not require heat and thus are applicable to functional groups and materials that decompose at high temperatures. Photochemical stimuli can also be employed as external stimuli to switch the reactions “on” and “off” and trigger the reactions locally at specific spaces and positions. Therefore, photoinduced CRP can widen a range of applicable monomers and open up novel applications to photolithography, for example. The reactions are also selectively inducible in response to the irradiation wavelengths, and thus multiple reactions may be regulated in one pot by conveniently varying the irradiation wavelength.

As mentioned above, the invention of RCMP was inspired by organic reactions in which an alkyl radical was reversibly generated from an alkyl halide with an amine. Interestingly, the literature reactions proceeded not only under heating but also under photoirradiation.³⁰ Besides, the RCMP process was generally induced by heating at high temperatures of 60–90 °C, which might inevitably arouse HI elimination especially at the later stage of polymerization. Therefore, it is sometimes difficult to efficiently achieve *in situ* chain extension and high molecular weight due to the low fraction of iodine chain ends. RCMP is encouraging for photocontrol in that various organic molecules can serve as catalysts, which exhibit different absorption wavelengths. These facts prompted Goto and Zhu *et al.* to explore photoinduced RCMP (photo-RCMP). Photo-RCMP involves only an alkyl iodide (dormant species) with or without an organic catalyst and uses visible light for irradiation. It is among the simplest, cheapest, and most robust photoinduced CRPs. It directly regulates reversible acti-



Scheme 5 Possible general mechanism of photo-RCMP.

vation without generating new chains in principle. In a general mechanism (Scheme 5), a complex of the dormant species and catalyst is initially formed and the C–I bond of the complex is subsequently photo-dissociated.

3.1. With the addition of a catalyst

In 2013, Goto's group studied the photo-RCMP at ambient temperature.³¹ The amines were employed as the catalyst, including PMDETA, TBA and TDEAP. They conducted UV–vis measurements, indicating that TBA and CPI had a peak at 290 nm and 280 nm, respectively, and their spectra ranged to about 400 nm. A new shoulder peak appeared for a mixture of CP-I and TBA at about 400 nm and ranged from 350 to 500 nm, which would correspond to a complex of CPI and TBA. Therefore, they used visible light at a wavelength of 350–600 nm. The radical trap experiment clearly demonstrates effective photolysis of CPI with TBA under visible light irradiation.

A bulk polymerization of MMA (8 M (100 equiv.)) with TBA (20 mM (0.25 equiv.)) and CPI (80 mM (1 equiv.)) was conducted under visible light irradiation (xenon lamp power = 60 W; wavelength = 350–600 nm), which proceeded up to a high monomer conversion of 80% in 5 h. The controllability of the polymerization was demonstrated by the first-order plot of the monomer concentration and the molecular weight data. The polymerization did not proceed smoothly without TBA, leading to only a low conversion (about 10%) and a large D (about 1.6) for 4 h, indicating that the observed successful photo-RCMP was due to the combination of CP-I and TBA. The elemental analysis of iodine suggested that the polymers obtained with TBA at 2 h (31% conversion), 3 h (47% conversion), and 4 h (67% conversion) contained high fractions, *i.e.*, 92%, 92%, and 90%, respectively (with $\pm 5\%$ experimental error), of the active polymer bearing iodine at the chain end. TDEAP and PMDETA also well worked as catalysts, producing low polydispersity polymers. PMDETA enabled even faster polymerization than TBA, which might be because the tri-amine PMDETA can more effectively coordinate iodine by wrapping iodine with multiple nitrogens. TDEAP had blue-shifted absorption (with a peak top of 350 nm) for the CPI/catalyst complex, which resulted in slower polymerization.

They systematically studied the effect of the irradiation power by fixing the concentrations of TBA (80 mM) and CPI (80 mM) and varying the lamp power (0–300 W). R_p was enhanced on increasing the lamp power; however, D became larger, suggesting side reactions at high power. Notably, no polymerization occurred without irradiation, demonstrating that the system is an ideal system switched “on” and “off” by external photoirradiation. The temporal control of the polymerization was confirmed by turning on and off the lamp

at every 30 min in four cycles. They also examined the synthesis of higher molecular weight polymers. Small D ($= 1.2\text{--}1.5$) values were achieved up to about 300 DPs ($M_n = \sim 30\,000$). However, D values became large on further increasing the DP in the studied cases. The photo-RCMP was compatible with various functional groups. Low polydispersity ($D = 1.1\text{--}1.4$) polymers were successfully obtained for some functional methacrylates with hydrophilic and hydrophobic functionalities such as hydroxyl (HEMA), poly(ethylene glycol) (PEGMA), dimethylamino (DMAEMA), epoxy (GMA), 2-ethylhexyl (EHMA), and benzyl (BzMA) groups.

Generally, the available systems of photo-CRP are confined in the wavelengths that can be used to control the polymerization. The feasible wavelength is nearly fixed in each system, which is fundamentally determined by the essential components (key elements and groups) present in the capping agents and catalysts. Greater versatility with respect to wavelength could be highly beneficial for widening the scope of photo-CRP. Goto *et al.* conquered this challenge concerning restricted wavelengths by employing various organic molecules with different absorption wavelengths as catalysts in photo-RCMP, which is feasible over a wide range of wavelengths, *i.e.*, 350–750 nm.³² They proposed a mechanism, in which the catalyst operates as an antenna that absorbs light and transfers the energy to cleave the C–I bond of the complex (Scheme 6). UV-vis-NIR spectra suggested that the mixtures of CPI with C1-DCI, DHMI, and C3-DCI exhibited longer absorption wavelengths, with the peak maxima located at 530, 600, and 720 nm, respectively. Thereby, longer wavelengths (>450 nm) could be employed to control the polymerization.

The bulk polymerizations of MMA (100 equiv.) containing CPI (1 equiv.) was carried out using C1-DCI (0.125 equiv.), DHMI (0.5 equiv.), or C3-DCI (0.25 equiv.) as a catalyst under irradiation at 550–750 nm. In all studied cases, the polymerization proceeded to a high monomer conversion (65–81%). No polymerization occurred without a catalyst, suggesting that the polymerization required both CPI and a catalyst. The control of M_n and D for these systems at 550–750 nm was as good as that for the TBA system at 350–600 nm, clearly demonstrating the successful extension of the feasible wavelength to a longer wavelength region. In addition to broad bands, narrow bands of wavelengths could also be efficiently employed. The poly-

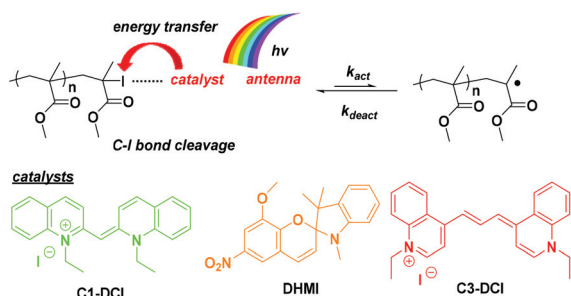
merizations at specific desired wavelengths of 400 (± 10) nm (TBA), 500 (± 10) nm (C1-DCI), 550 (± 10) nm (DHMI), 600 (± 10) nm (DHMI), and 700 (± 50) nm (C3-DCI) were well-controlled. Compared with the R_p of the broad-band systems, the R_p in these cases was smaller due to the lower irradiation intensities (narrower bands). The system was switched “on” and “off”, and R_p was finely tuned by altering the absorption intensity at each wavelength. These catalysts are amenable to several functional methacrylates with hydroxyl (HEMA), poly(ethylene glycol) (PEGMA), 2-ethylhexyl (EHMA), epoxide (GMA), and dimethylamino (DMAEMA) groups.

As mentioned in the previous section, the polymerization by pyridine *N*-oxide catalysts could be controlled by thermal heating.²⁷ The polymerization also proceeded well under photoirradiation. The polymerization of MMA (8 M, 100 equiv.) with PPD-PO (20 mM, 0.25 equiv.) and CPI (80 mM, 1 equiv.) was performed under LED (light-emitting diode) irradiation (380–550 nm) at ambient temperature (20 °C). This system is an excellent photo-switchable polymerization, affording low-dispersity ($D = 1.09\text{--}1.20$) polymers with M_n up to 28 000. ¹H NMR was employed to analyse the chain-end of the PMMAs obtained under thermal conditions ($M_n = 1800$ and $D = 1.12$) and photoconditions ($M_n = 2000$ and $D = 1.16$), respectively. The polymer obtained under the thermal conditions contained 59% iodide at the growing chain-end (with $\pm 5\%$ experimental error). In contrast, the polymer produced under the photoconditions possessed 98% iodide with an error range of 93–100%. The side reaction was greatly suppressed probably due to the decreased temperature (20 and 70 °C for the photo- and thermal conditions, respectively). Exploiting the living character, they carried out block polymerizations using macroinitiators produced under photoirradiation because of the high iodide chain-end fidelities. Using purified PMMA-iodide (PMMA-I) macroinitiators ($M_n = 4200$ and $D = 1.10$ and $M_n = 4700$ and $D = 1.09$), the thermal polymerizations of PEGMA and BzMA yielded hydrophobic–hydrophobic and hydrophobic–hydrophilic block copolymers, *i.e.*, PMMA-*b*-PPEGMA and PMMA-*b*-PBzMA.

3.2. Catalyst-free polymerization systems

Over the past few years, LED technology has been developed. In particular, the adjusting-illumination technology in the visible spectrum holds great promise for the medicine, biotechnology, as well as photo-polymerization areas because of its characteristic virtues such as no ozone release, low energy consumption, low heat generation, high performance, simple and safe operation, cost-effectiveness, *etc.* In addition to the light source influence, atom economical and environmentally benign strategies have been proposed to develop sustainable and green systems, such as recyclable,³³ metal-free,^{34,35} or even catalyst-free polymerization systems. It is obvious that catalyst-free polymerizations are more attractive due to their advantages of environmentally friendly, atom economical and cost-effective features.

In 2016, Zhu *et al.* reported the photo-induced CRP of methacrylates without the addition of any metals, additive



Scheme 6 C–I bond cleavage of polymer iodide *via* light absorption of the catalyst (antenna) and subsequent energy transfer.

agents or special catalysts.³⁶ Mechanistically, the polymerization process and its controllability were mediated with the assistance of solvents through the reversible photo-cleavage of the C–I bond and the formation of dormant species. This system was also an ideal “on–off” switchable system upon an external sequential photo-stimulus. Under white LED irradiation (400–720 nm, $\lambda_{\text{max}} = 440, 540$ nm), the conventional solvent was screened at a target polymerization degree of 100 for 12 h. In bulk polymerization of MMA and polymerization in anisole, toluene or dioxane, the photo-dissociation efficiencies of the C–I bond of the dormant species and the monomer conversions were very low ($\leq 10\%$). However, when DMF, dimethyl sulfoxide (DMSO), or *N,N*-dimethylacetamide (DMAC) was used as the solvent, much higher conversions were achieved (56–92%). It was found that the molecular weight and polydispersity were all well-controlled in various solvents (including bulk polymerization).

They proposed that DMF, DMSO or DMAC maybe could more effectively coordinate iodine to initially form a complex of dormant species with the solvent, and the activation of the C–I bond was subsequently promoted with the assistance of the solvent under photoirradiation, which agrees with the general mechanism of RCMP (Fig. 8). PMMA produced in DMSO exhibited a lower molecular weight than the theoretical value with a slightly broader distribution ($M_w/M_n = 1.23$), demonstrating that effective initiation proceeded, yet dead polymerization chains due to side reactions could not be ignored. Polymerization in DMAC afforded a relatively high conversion (83.6%) and low molecular weight distribution ($M_w/M_n = 1.16$). UV-vis absorption analysis suggested that the coordination of the formed iodine with DMAC contributed to a wide spectral wavelength scope extended to ~ 690 nm; thereby, polymerization reactions could take place over a wide range of wavelengths. Under green light irradiation with moderate wavelength and energy density, the polymerization rate was rapid and maintained good control over the molecular weight in many cases. Therefore, under green LED light irradiation, the compatibility of the catalytic system with functional monomers was studied. Some hydrophilic and hydrophobic functional methacrylates such as PEGMA, glycidyl methacrylate (GMA), HEMA and benzyl methacrylate (BnMA) were successfully produced with narrow molecular weight distributions ($M_w/M_n = 1.05$ – 1.25).

The above results illustrate that the photocleavage of the carbon–iodine bond of organoiodine compounds with the

assistance of specific polar solvents is an attractive strategy for designing novel catalyst-free iodine-mediated polymerization systems. However, the use of the polar solvent not only reduces the polymerization rate but also increases the cost. Therefore, it is quite ideal to explore simpler CRP systems with just two components (a monomer and a mediator). Based on a similar role of functional monomers with epoxy, amine and ethoxyl groups as polar solvents, Zhu *et al.* successfully explored a simple and highly efficient visible-light induced iodine-mediated controlled radical polymerization system for functional monomers (PEGMA, DMAEMA and GMA) in bulk without any catalysts.³⁷ Under blue LED irradiation (4.8 W, $\lambda_{\text{max}} = 464$ nm), the photoinduced bulk LRP was first attempted for the polymerization of DMAEMA using CPI as a photo-initiator and the reaction system was kept at ambient temperature with magnetic stirring for the desired time. The polymerizations were well controlled with narrow molecular weight distributions ($M_w/M_n = 1.19$ – 1.34). The bulk polymerizations of PEGMA at a DP of 50 could also proceed under blue LED irradiation with good control ($M_w/M_n = 1.09$ – 1.17). However, the GPC elution curves at higher monomer conversions ($>71.9\%$) were no longer as unimodal as those at low conversions because of coupling termination from a small portion of propagating radicals (polymer \cdot). They conducted the visible-light induced bulk CRP of GMA, in which the $M_{n,\text{GPC}}$ increased linearly with monomer conversion, and the molecular weight distributions of the obtained polymers were narrow (1.04–1.14).

The photoinduced CRP by direct use of sunlight has a great advantage over the traditional polymerization engineering. Photoinduced bulk CRP of PEGMA, DMAEMA or GMA using CPI as an initiator could be performed by direct exposure to sunlight without any optical filters. The applicability of the catalyst-free bulk CRP methodology to other monomers such as BnMA, MMA, and HEMA was also investigated. PBnMA and PMMA were obtained with very low monomer conversions for 18 h of blue LED irradiation. In the case of PHEMA, broader molecular weight distributions and inevitable coupling terminations were observed. The above experimental results demonstrate that the construction of this bulk CRP system must rely on the coordination of organoiodine components and monomers with specific functional groups, which conforms to RCMP (Fig. 9). GMA, DMAEMA and PEGMA can not only work as monomers, but also serve to coordinate with CPI to activate and control the polymerization under visible light irradiation

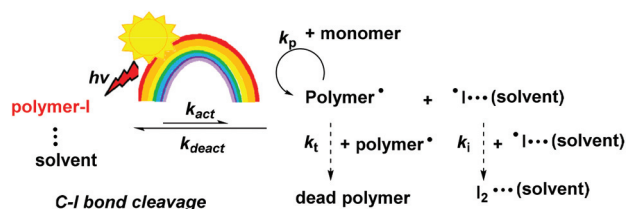


Fig. 8 Proposed mechanism for the catalyst-free iodine-mediated CRP.

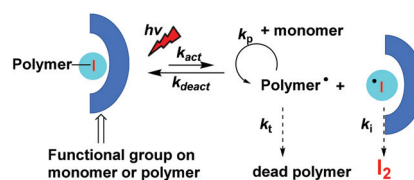


Fig. 9 Proposed polymerization mechanism of catalyst-free iodine-mediated bulk CRP of functional monomers.

by virtue of the presence of functional glycidyl, amino and ethylene glycol groups.

Short-wavelength light can cause safety concerns and considerably interfere with the potential applications, as it can be absorbed by lots of common compounds and usually causes some unpredictable side reactions.³⁸ Besides, high-energy light sources suffer from a lack of high penetration depth. Therefore, some long-wavelength (>700 nm) sensitized photocatalysts for CRPs have been explored, though not extensively. As mentioned above, Goto and coworkers reported RCMP in the presence of long-wavelength light by exploiting 1,1-diethyl-4,4'-carbocyanine iodide (C3-DCI) as the catalyst.³² Besides, a near-infrared (NIR) photo-induced RAFT polymerization system has also been developed. For instance, Boyer *et al.* employed an expensive bacteriochlorophyll a (BChl a) as the photoredox catalyst to trigger photoinduced electron transfer (PET)-RAFT polymerization in the NIR light region.³⁹

As we all know, an alkyl iodide (RI) has a weak C–I bond. It has been reported that homolytic dissociation energies for CPI and EIPA in the solvent DMF at 298.15 K are 153.4 kJ mol⁻¹ and 143.1 kJ mol⁻¹, respectively. In contrast, according to the second law of actinchemistry, the energies for the 750–680 nm range of irradiation wavelengths are estimated as 159–176 kJ mol⁻¹. Therefore, it is obvious that NIR light energy could cleave the C–I bonds of these alkyl iodides. Based on this possibility, Zhu *et al.* successfully developed a new facile NIR photocontrolled polymerization system for various methacrylates by photocatalyst-free iodine-mediated CRP upon irradiation with 730 nm LED light by using a series of special solvents bearing carbonyl groups (referred to as carbonyl solvents in short), such as urea-type solvents (tetramethylurea (TMU), 1,3-dimethyl-2-imidazolidinone (DMI), and 1,3-dimethyl-tetrahydropyrimidin-2(1*H*)-one (DMPU), and amide-type solvents [*N*-methyl pyrrolidone (NMP) and *N,N*-dimethylacetamide (DMAc)], as both the solvent and catalyst.⁴⁰ The polymerization of MMA was conducted either in bulk or in various solvents (*e.g.*, acetonitrile, DMSO, ethanol, tetrahydrofuran (THF), 1,4-dioxane, chloroform, toluene and anisole) upon irradiation with 730 nm LED light at room temperature (25 °C). However, relatively low monomer conversions were achieved (<36%) after 18 hours. The monomer conversions increased significantly (more than 56%, up to 98%) by using carbonyl solvents such as DMI, TMU, DMPU, DMAc, and NMP under the same reaction conditions, and the resultant PMMAs were obtained with narrow molecular weight distributions ($M_w/M_n = 1.04\text{--}1.12$). They also explored the catalytic effects of other types of solvents containing a carbonyl group, which demonstrated that the inductive electron contribution of the two substituent groups to the carbonyl group of the carbonyl solvents is the critical reason for successful NIR photo-CRP.

The polymerization of MMA was conducted in different noncarbonyl solvents with a molar ratio of $[MMA]_0/[CPI]_0/[DMI]_0 = 164 : 1 : 1$. The monomer conversion was rather low in low-polarity solvents (*e.g.*, anisole and toluene), even with the addition of a catalytic amount of DMI. But the experimental results varied significantly in high polarity solvents. By adding

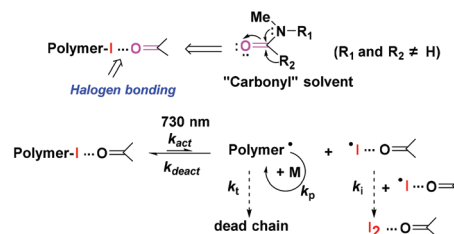
a catalytic amount of DMI into DMSO, high conversion (92%) and narrow molecular weight distribution ($M_w/M_n = 1.15$) were achieved upon irradiation with 730 nm light for 18 hours, meaning that this polymerization system became well-controlled in comparison with that without DMI. Based on the above experimental results, it can be concluded that the interaction (reversible complexation) of a specific carbonyl solvent with an iodine reagent is important for a successful NIR photocontrolled iodine-mediated CRP, which can get pigeonholed as RCMP. The mechanism is proposed in Scheme 7.

Due to its high penetration performance, the NIR photocontrolled CRP of MMA in a vessel shielded by translucent bio-tissue barriers, for example, the skin of pork, was successfully conducted. When either 1.0 or 2.0 mm thick pork skin was employed, a high monomer conversion (81%) was achieved after 21 hours, demonstrating the excellent tissue penetration ability of 730 nm light. Besides, they also investigated the polymerization behaviour by penetrating multiple layers of A4 paper with a 0.1 mm thickness of each layer. Even when shielded by three layers of A4 paper (0.3 mm), the polymerization achieved a 53.3% monomer conversion and polymers with narrow molecular weight distribution ($M_w/M_n = 1.07$), fully illustrating the unique advantages of this facile NIR photocontrolled CRP.

3.3. Bromine-iodine transformation

Goto *et al.* have made great contributions to iodine transfer polymerizations and have applied a variety of organic catalysts for photo-RCMP. However, the unstable iodine-containing initiators with weak C–I bonds are light- and heat-sensitive to be decomposed by elimination reactions under storage. Goto⁴¹ and Zhu⁴² *et al.* developed a new methodology, termed “bromine-iodine transformation activated living radical polymerization”, building a “bridge” between ATRP and RCMP techniques. This strategy is based on the *in situ* synthesis of iodinated species *via* the nucleophilic substitution reaction as an internal boost, which eliminates the preliminary synthesis and storage of the iodinated compounds.

In 2017, Goto and coworkers used halogen exchange of alkyl bromide (R–Br) with NaI to generate alkyl iodide (R–I) *in situ*, which was employed as an initiating dormant species of RCMP.⁴¹ They found that the R group of R–Br significantly affects the efficiency of the transformation. By the rational



Scheme 7 Proposed polymerization mechanism of NIR photocontrolled iodide-mediated CRP using carbonyl solvents as both the catalyst and solvent.

selection of the reaction temperature and R–Br along with the use of Bu_4NI as a catalyst, well-controlled polymerizations of methacrylates, BA, styrene, and acrylonitrile were achieved with high conversions (e.g., 70–90%) in relatively short periods of time (typically 3–10 h). Besides, a chain-end functional polymer and well-defined deblock and triblock copolymers were obtained. The use of simple, stable, and inexpensive R–Br as precursors is an attractive feature of this system, as various R–Br are commercially available and R–Br are generally much more stable than R–I upon storage. This work demonstrated the high monomer versatility and the accessibility to a wide range of polymer structures, showing the capability of this system of use in a range of applications.

In the same year, Zhu *et al.* reported a facile and effective visible-light-induced CRP system at room temperature by using typical alkyl bromides (such as 2-bromopropanenitrile (BPN) and ethyl α -bromophenylacetate (EBPA)) as the initiator with the addition of NaI.⁴² Water-soluble PEGMA was used as the model monomer. The optimized polymerization conditions were established by investigating the influencing factors including the initiator and solvent type, activator (sodium iodide) and catalyst (triethylamine) concentration, solvent volume, light source, and degree of polymerization (DP). Excellent control over the molecular weights of the polymers was achieved under LED irradiation. Without adding any sodium iodide, no polymerization occurred at all. A less proportion of sodium iodide was utilized (0.1–1.0 equivalent), the molecular weight distributions were wide with poor control and the monomer conversions were relatively low. The molecular weight and monomer conversion gradually tended to be stabilized, achieving a relatively satisfactory degree when the usage of sodium iodide was more than 1.0 equivalent. Besides, in the presence of TEA as the catalyst, the moderate polymerization rate could be drastically promoted. This polymerization system showed instantaneous control in response to the on–off switch of the irradiation stimulus. Other monomers (such as GMA and MMA) also proved to be compatible with this CRP system.

The possible polymerization mechanism was investigated. Without the addition of any sodium iodide, no polymerization occurred even when TEA was added, demonstrating that the activation and controllability of polymerizations were caused by NaI. In the presence of NaI, no polymer was produced without any initiator, indicating that NaI directly reacted with the initiator to activate the polymerization. In complete darkness, no polymerization took place as well; thus, the reactions were strictly driven by the light-exposure as an external stimulus. These control experiments showed that the removal of any specific component (EBPA or BPN, NaI, and light source) should not provide any polymeric products. As shown in Fig. 10, the catalyst TEA can effectively coordinate with the dormant species (polymer-I) to form a complex (polymer-I/TEA) initially, and the dissociation of the light-sensitive C–I bond of polymer-I was then activated upon light-exposure. Subsequently, the formed radical (polymer \cdot) triggered orderly chain propagation, and the dynamic activation–deactivation

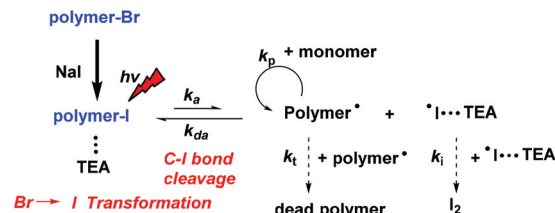


Fig. 10 Proposed polymerization mechanism of photo-induced and bromine–iodine transformation activated CRP.

equilibrium was established. The I \cdot /TEA radical was so active that it tended to recombine with another one to generate free iodine (I_2) in the polymerization medium, which was confirmed by UV-vis absorption spectroscopic analysis.

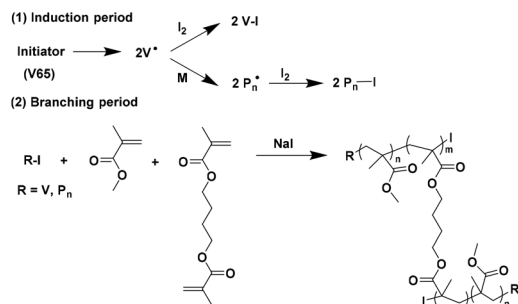
4. Applications

Unlike living anionic polymerization, RCMP does not require stringent removal of moisture and also is a metal- and odor-free polymerization. It is amenable to a range of monomer and polymer designs. Besides, photo-RCMP is controllable over the whole range of visible-light wavelengths. RCMP is considered a powerful method for polymer synthesis, owing to its inexpensive, non-toxic and easy-to-handle catalyst. Next, we will briefly introduce the applications of RCMP in the aspects of topology design, self-assembly, surface modification and dispersity control, which were mainly investigated by Goto and Jiang *et al.*

4.1. Topology design and self-assembly

Highly branched polymers have become a most promising type of polymer because of their divergent three-dimensional globular structure and their large number of terminal functionalities.⁴³ As a result of these unique structural properties, they exhibit lower viscosity and greater solubility compared with their linear analogues and are suitable candidates for use in catalysis, drug delivery, gene carriers and viscosity modifiers.⁴⁴ Jiang *et al.* reported the reversible complexation-mediated copolymerization (RCMCP) of vinyl and divinyl monomers for the synthesis of highly branched polymers.⁴⁵ A free-radical polymerization inhibitor (I_2), a conventional azo radical initiator V65, and a highly reactive but inexpensive salt (NaI) were used to initiate and control the polymerization (Scheme 8). The most significant branching occurred when the conv. MMA approached 90% due to intermolecular reactions between macromolecules. The polymerization reaction can also be performed without deoxygenation, and no obvious prolongation of induction was observed.

ABC-type miktoarm star copolymers are star polymers bearing three arms with different monomer compositions. In polymer science, they are advanced branching architectures and offer unique assembly structures that are useful for drug/gene delivery, for example. In 2020, Goto *et al.* synthesized ABC-type miktoarm star copolymers employing RCMP.⁴⁶ Their



Scheme 8 Simplified mechanism for the formation of a highly branched copolymer *via* RCMCP.

approach uses a single CRP technique (RCMP) and is classified as a “combinatorial” approach. Different from the “core-first” and “coupling-onto” approaches, the “combinatorial” approach does not require the pre-synthesis of special multi-initiating or multi-coupling core molecules that are meticulously designed to avoid the interference of each initiation or coupling reaction. The “combinatorial” approach also does not require stringent anionic polymerization. Fig. 11 shows the synthetic procedure. They synthesized polymer A (first arm) with an iodinated chain end and transformed the iodide to a reactive vinyl group. Polymer B (second arm) is subsequently connected to the reactive vinyl group to generate block copolymer AB with an iodide at the junction. The junction initiates the growth of polymer C (third arm) and forms the star terpolymer ABC. RCMP is utilized for the synthesis of the A, B, and C arms. Polymer A (first arm) is poly(butyl acrylate) (PBA), and polymer B (second arm) is poly(methyl methacrylate) (PMMA). Polymer C (third arm) encompassed different polymers, that is, poly(2-methoxyethyl acrylate) (PMEA), poly(2-phenoxyethyl acrylate) (PPEA), and PPEGA.

In 2018, they designed an alkyl diiodide ($I-R^2-R^1-I$; Fig. 12) with considerably different reactivities of R^1-I and $I-R^2$; thus, it can selectively initiate at a given temperature (from R^1-I) and an elevated temperature (from $I-R^2$).⁴⁷ Interestingly, this initiator enables the synthesis of non-symmetric CABC multi-block copolymers. At a mild temperature, two monomers A and B are successively polymerized from R^1-I , whereas $I-R^2$ remains intact. Monomer C is subsequently polymerized at an

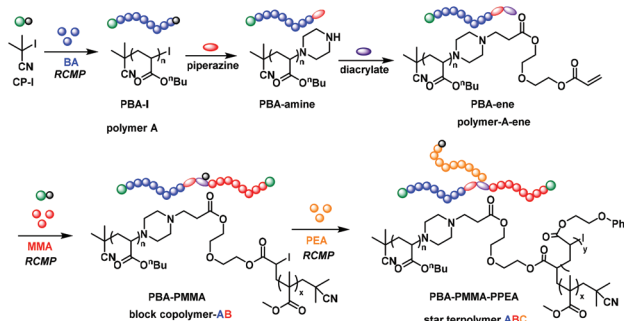


Fig. 11 Synthetic procedure of an ABC miktoarm star copolymer.

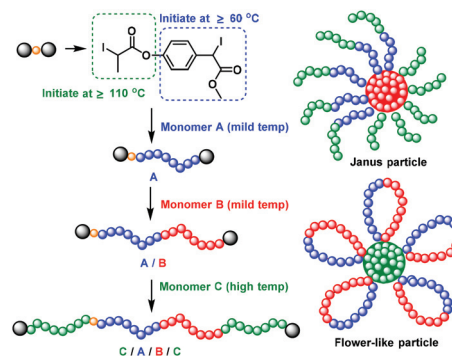


Fig. 12 Temperature-selective polymerization for synthesis of a CABC multi-block copolymer.

elevated temperature, whereupon propagation takes place from both chain ends. CABC block copolymers are thus produced by simply altering the temperature. Diblock, triblock, and multi-block copolymers have garnered increasing attention owing to their assembly structures. Based on the non-symmetric structure of the CABC block copolymer, a Janus-type particle with heterosegment coronas and a flower-like particle with heterosegment petals were synthesized as unique applications. For the Janus-type particle, the B segment is cross-linked to form a particle with two distinguishable homo-C-segment and hetero-CA-segment coronas. For the flower-like particle, a particle with hetero-AB-segment petals forms *via* the crosslinking of the C segment.

The morphological transformation of polymer nanoparticles, in which the particle structures reversibly change in response to external stimuli such as light, temperature, and pH, has attracted great attention for various smart responsive materials in, for example, fluorescent thermometers, biosensors, and drug-delivery applications.⁴⁸ Such morphological transformations enable the control of the physicochemical properties of the nanoparticles such as optical, rheological, encapsulation, and bio-interaction properties. In 2020, Goto's group employed CABC block copolymers to create novel micellar morphological transformation systems.⁴⁹ The nanostructures are reversibly switched from Janus-type star micelles to symmetric flowerlike micelles *via* altering the temperature (Fig. 13a). Block A is a hydrophobic segment (blue), block B is a hydrophilic segment (red), and block C is thermosensitive (green) having a lower critical solution temperature (LCST) in water. Below the LCST, block C is soluble in water. Therefore, only block A is insoluble to form a core, which is expected to give a Janus-star micelle with blocks C and BC in the shell. Above the LCST, block C is insoluble in water. Blocks A and C are insoluble to form a core to give a flower micelle with block B in the shell (petal). To form the flower as expected, blocks A and C should be well compatible. This type of star-flower transformation is achievable by combining a hydrophilic block B to retain the shell, a hydrophobic block A to retain the core, and a thermosensitive block C to switch the morphology, and thereby is unique to CABC block copolymers. The physico-

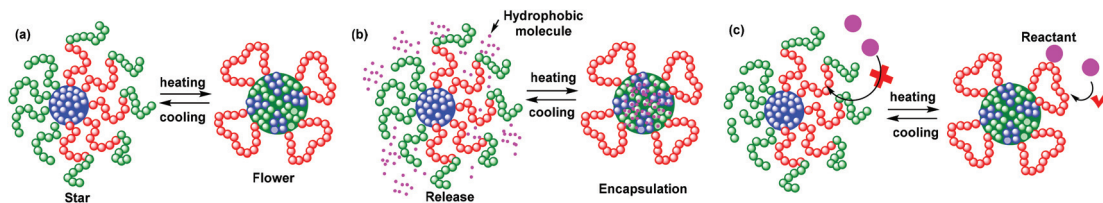


Fig. 13 (a) Reversible morphological transformation between a star micelle and a flower micelle self-assembled by a CABc multiblock copolymer. (b) Reversible encapsulation and release of external hydrophobic molecules. (c) Hidden and exposed functional segments.

chemical properties of the nanostructures can be tuned with star–flower transformations. The large difference in the core size between the star and flower can greatly change the loading capacity in the core (Fig. 13b) and is expected to afford the reversible encapsulation and release of external molecules. The hidden functional segment is another interesting application. Block B (red segment) is expected to be shielded (hidden) in the star by block C (green segment) (Fig. 13c). Block B is expected to be exposed upon heating, due to the transformation to the flower. The hidden segment can interact with external molecules or surfaces, which provides a novel interface on the nanostructure.

4.2. Surface modification

Surface modification on nano- and microscales is of great importance for various applications in bio-microarrays, microelectronics, microfluidic systems, and so on.⁵⁰ The fabrication of polymer brushes (PBs) on surfaces is an efficient strategy for endowing the functional surfaces with improved properties.⁵¹ Patterned PBs have been obtained by surface-initiated controlled radical polymerization from pre-patterned initiators. A binary PB, which serves as a smart or stimuli-responsive surface, is composed of two different PBs tethered on a surface.⁵² Binary PBs in a patterned manner are pretty attractive and may find new applications in micro-electromechanical materials and functional coatings, for example. However, there have been only a few examples of patterned binary PBs, mainly due to their complicated fabrication processes such as multi-step immobilization of initiators.⁵³

In 2018, Goto *et al.* reported photo-controlled surface-initiated RCMP for the fabrication of complex patterns of PBs with high density.⁵⁴ Patterned PBs were obtained using photo-masks under visible light (550 ± 50 nm), yielding positive patterning (Fig. 14a). A unique aspect of RCMP is the use of the RI initiator, which is advantageous for degradation owing to the weak carbon–iodide bond. They found that the surface immobilized R–I could completely degrade in under 1 minute of UV radiation with a nonspecial UV source (≥ 250 nm). This finding enabled the convenient preparation of pre-patterned initiator surfaces eliminating the need for special equipment or techniques such as vacuum-UV lithography (≤ 200 nm wavelength). Thus, PBs grew from the nondegraded initiators, yielding negative patterning (Fig. 14b). The combination of positive and negative patterning further provides a novel synthetic

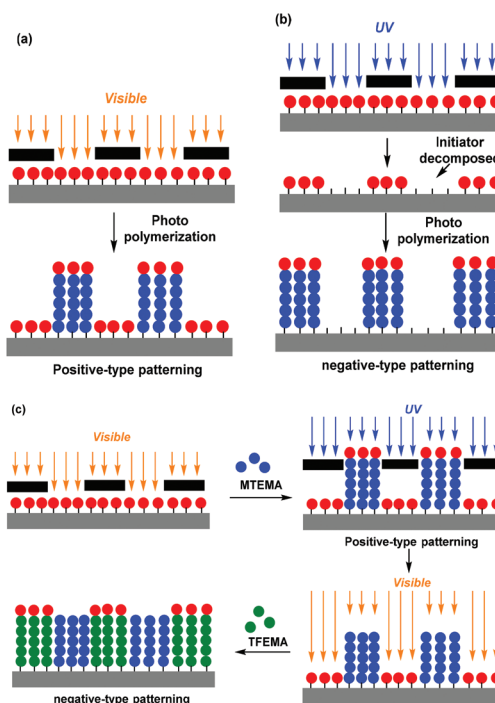


Fig. 14 (a) Illustration of positive patterning of poly(benzyl methacrylate) (PBzMA) brushes; (b) negative patterning of PBzMA brushes; and (c) the synthesis of patterned binary PBs.

technique of patterned binary PBs (Fig. 14c), which uses only a single initiator in a one-step immobilization process.

The graft density (surface occupancy (σ^*)) dramatically changes the conformation of the brush polymer in a solvent.⁵⁵ At low graft densities ($\sigma^* \leq 1$ –2%, typically), diluted polymer brushes will assume a mushroom conformation. By increasing the graft density, graft chains will overlap with each other and are obliged to stretch away from the surface. Patterned polymer brushes with different graft densities are very interesting, as polymer brushes with different physical properties are arranged in two-dimensional (2D) or three-dimensional (3D) patterns.

4.3. Dispersity control

The molecular weight distribution of polymers is a fundamental parameter for determining polymer properties such as viscoelasticity, processability, and self-assembly behaviors. CRP enables the synthesis of polymers with small D values, pre-

determined molecular weights and sophisticated architectures. However, polymers with large D values are sometimes desired for improved physical properties such as processability and miscibility. The manipulation of D in CRP is very important but still challenging.

The R group determines the rate of the generation of R^{\cdot} . The R-I bond for the R = acrylate polymer (with a secondary alkyl chain end) is significantly stronger than that for the R = methacrylate polymer (with a tertiary alkyl chain end). Therefore, a mild temperature (e.g., 60–70 °C) is sufficient for the methacrylate polymerizations, while an elevated temperature (e.g., 110 °C) is required for the acrylate polymerizations. Goto's group further employed this temperature selectivity to develop a novel strategy to modulate D .^{56,57} In the method, a small amount of BA is used in an RCMP of MMA at a mild temperature. Once a propagating radical possessing BA at the terminal unit is capped with iodide, the resultant polymer-iodide could hardly reinitiate at the mild temperature. During the polymerization, the BA-terminal dormant species gradually accumulate, which results in increased D (Fig. 15). Thus, the amount of BA modulates the amount of the accumulated BA-terminal dormant species (and hence D). The D value can be tuned in any segment of linear and branched block copolymers without segmental or topological restriction. This strategy is also amenable to heterogeneous systems such as polymer brush synthesis. The unique D -dependent size exclusion effect of the polymer brush may open up novel functional interfaces for sensing and biological applications.

5. Summary and outlook

In summary, RCMP is environmentally friendly and acts as an ideal method for the synthesis of metal-free polymer materials with low toxicity. There are several other metal-free controlled radical polymerizations, mainly including nitroxide mediated polymerization (NMP),⁵⁸ reversible addition-fragmentation chain transfer (RAFT) polymerization,⁵⁹ and organocatalyzed atom transfer radical polymerization (O-ATRP).⁶⁰ Each of these polymerization methods features different advantages and disadvantages relative to RCMP. NMP typically performed in the absence of a catalyst and sometimes without the addition of an initiator, which could avoid the tedious polymer purification. However, most of the alkoxyamines are not commercially available and must be synthesized with high cost prior to the polymerization. The greatest advantage of RAFT is the wide

range of monomers. In addition to common monomers, acidic and alkaline monomers can be easily polymerized, which is very conducive to the preparation of materials containing special functional groups. Although some of the RAFT chain transfer agents are now commercially available, they are generally more expensive than the alkyl halide initiators. Dithiester derivatives may increase the toxicity of the polymer and can impart color and odor to the polymers. As with NMP, initiators are usually required to generate radicals in RAFT polymerization, which tends to cause chain termination. O-ATRP typically uses commercially available reagents, and is an excellent method for the precise polymerization of various monomers, including methacrylates, acrylates, styrene, and vinylcyclopropanes. However, it is challenging for the current O-ATRP methods to synthesize high molecular weight polymers, and they usually produce polymers with $M_n \sim 1\text{--}50 \text{ kg mol}^{-1}$. Besides, it is difficult to expand the range of irradiation wavelengths that can be employed in photo-induced O-ATRP to longer wavelengths.

In the context of other metal-free CRPs, RCMP has been developed as a new class of CRP using organic catalysts. The molecular weights and their distribution were well controlled in the polymerizations of MMA, St, AN, and some functional methacrylates. The RCMP system includes no conventional radical initiator (being different from NMP and RAFT polymerization). The catalysts include tertiary amines, iodide anions, pseudohalide anions, oxyanions, and special solvents. In particular, photo-RCMP involves only an alkyl iodide (dormant species) with or without a catalyst (being different from photo-induced RAFT polymerization and O-ATRP). It is among the simplest, cheapest, and most robust photoinduced CRPs. Similar to RAFT polymerization, the feasibility of RCMP over the whole visible region and near-infrared region is very attractive, which is challengeable for NMR and O-ATRP. The low cost, good environmental safety, ease of handling and compatibility with various functional groups of the RCMP system are highly attractive for practical applications. However, RCMP has important limitations, particularly with respect to monomer versatility and molecular weight. The molecular weight is limited to 10^4 in most cases (like O-ATRP). The efficient controlled polymerizations of acrylates, (meth)acrylic acid, St and AN are difficult to attain for photo-RCMP, which have not been reported so far. On the other hand, in addition to topology as well as molecular weight and its distribution, the physical, chemical and processing properties of polymers are greatly affected by the stereo-structures of polymer chains. The high activity and nearly planar structure of alkyl radicals make it a great challenge to realize stereospecificity in RCMP, just as in the cases of other radical polymerizations, and the stereospecific RCMP has not been reported so far. To cope with these challenges, novel catalytic systems need to be further developed. Through the dual optimization of the catalyst structure and reaction conditions, it is promising to achieve better regulation over the reversible activation-dormancy process, and significant impact on the stereo-chemistry of the polymerization process. Therefore, efficient and stereotactic RCMP

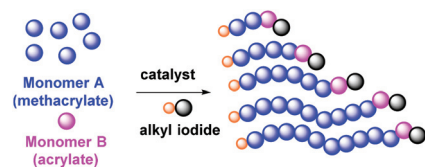


Fig. 15 Synthesis of a polymer with high dispersity and high iodide chain-end fidelity.

could be realized, producing polymers with ultrahigh molecular weight and/or high tacticity, which might greatly expand the potential applications of the RCMP polymer. The corresponding research is under way in our group.

Conflicts of interest

The authors declare no conflict of interest.

Acknowledgements

The authors are grateful for financial support by the Youth Innovation Promotion Association CAS (No. 2020259), the National Natural Science Foundation of China (21901253 and U19B6001), and Shanghai Rising-Star Program (21QA1411200).

Notes and references

- J. Nicolas, Y. Guillaneuf, C. Lefay, D. Bertin, D. Gigmes and B. Charleux, *Prog. Polym. Sci.*, 2013, **38**, 63–235.
- M. Ouchi, T. Terashima and M. Sawamoto, *Chem. Rev.*, 2009, **109**, 4963–5050.
- F. di Lena and K. Matyjaszewski, *Prog. Polym. Sci.*, 2010, **35**, 959–1021.
- G. Moad, E. Rizzardo and S. H. Thang, *Aust. J. Chem.*, 2009, **62**, 1402–1472.
- K. Matyjaszewski and N. V. Tsarevsky, *J. Am. Chem. Soc.*, 2014, **136**, 6513–6533.
- X.-Y. Wang, X.-L. Sun, F. Wang and Y. Tang, *ACS Catal.*, 2017, **7**, 4692–4696.
- S. Schaubach, X.-Y. Wang, J.-F. Li, X.-L. Sun, S. R. Wang and Y. Tang, *Polym. Chem.*, 2018, **9**, 4711–4715.
- X.-Y. Wang, X.-L. Sun, Z.-H. Chen, F. Wang, S. R. Wang and Y. Tang, *Polym. Chem.*, 2018, **9**, 4309–4315.
- X. Y. Wang, Z. H. Chen, X. L. Sun and Y. Tang, *Polymer*, 2019, **178**, 121630.
- Z.-H. Chen, X.-Y. Wang, X.-L. Sun, J.-F. Li, B.-H. Zhu and Y. Tang, *Macromolecules*, 2019, **52**, 9792–9798.
- N. J. Treat, H. Sprafke, J. W. Kramer, P. G. Clark, B. E. Barton, J. Read de Alaniz, B. P. Fors and C. J. Hawker, *J. Am. Chem. Soc.*, 2014, **136**, 16096–16101.
- X. Pan, C. Fang, M. Fantin, N. Malhotra, W. Y. So, L. A. Peteanu, A. A. Isse, A. Gennaro, P. Liu and K. Matyjaszewski, *J. Am. Chem. Soc.*, 2016, **138**, 2411–2425.
- A. Goto, T. Suzuki, H. Ohfuji, M. Tanishima, T. Fukuda, Y. Tsujii and H. Kaji, *Macromolecules*, 2011, **44**, 8709–8715.
- Y. Ni, L. Zhang, Z. Cheng and X. Zhu, *Polym. Chem.*, 2019, **10**, 2504–2515.
- C.-G. Wang, A. M. L. Chong, H. M. Pan, J. Sarkar, X. T. Tay and A. Goto, *Polym. Chem.*, 2020, **11**, 5559–5571.
- N. V. Tsarevsky and B. S. Sumerlin, *Fundamentals of Controlled/Living Radical Polymerization*, Royal Society of Chemistry, London, UK, 1st edn, 2013.
- K. Matyjaszewski and M. Möller, *Polymer Science: A Comprehensive Reference*, Elsevier, Amsterdam, the Netherlands, 1st edn, 2012.
- W. X. Wang, L. J. Bai, H. Chen, H. Xu, Y. Z. Niu, Q. Tao and Z. P. Cheng, *RSC Adv.*, 2016, **6**, 97455–97462.
- L. Lei, M. Tanishima, A. Goto and H. Kaji, *Polymers*, 2014, **6**, 860–872.
- B. Li, Y. Shi and Z. F. Fu, *J. Polym. Sci., Part A: Polym. Chem.*, 2019, **57**, 1653–1663.
- A. Goto, A. Ohtsuki, H. Ohfuji, M. Tanishima and H. Kaji, *J. Am. Chem. Soc.*, 2013, **135**, 11131–11139.
- A. Goto, T. Terauchi, T. Fukuda and T. Miyamoto, *Macromol. Rapid Commun.*, 1997, **18**, 673–681.
- C.-G. Wang, F. Hanindita and A. Goto, *ACS Macro Lett.*, 2018, **7**, 263–268.
- C. G. Wang, X. Y. Oh, X. Liu and A. Goto, *Macromolecules*, 2019, **52**, 2712–2718.
- J. Sarkar, L. Q. Xiao and A. Goto, *Macromolecules*, 2016, **49**, 5033–5042.
- C. G. Wang and A. Goto, *J. Am. Chem. Soc.*, 2017, **139**, 10551–10560.
- H. Xu, C.-G. Wang, Y. Lu and A. Goto, *Macromolecules*, 2019, **52**, 2156–2163.
- W. Mao, C.-G. Wang, Y. Lu, W. Faustinelie and A. Goto, *Polym. Chem.*, 2020, **11**, 53–60.
- Y. A. Wang, Y. Shi, Z. F. Fu and W. T. Yang, *Polym. Chem.*, 2017, **8**, 6073–6085.
- H. Ishibashi, S. Haruki, M. Uchiyama, O. Tamura and J.-I. Matsuo, *Tetrahedron Lett.*, 2006, **47**, 6263–6266.
- A. Ohtsuki, A. Goto and H. Kaji, *Macromolecules*, 2013, **46**, 96–102.
- A. Ohtsuki, L. Lei, M. Tanishima, A. Goto and H. Kaji, *J. Am. Chem. Soc.*, 2015, **137**, 5610–5617.
- L. J. Bai, L. F. Zhang, J. L. Pan, J. Zhu, Z. P. Cheng and X. L. Zhu, *Macromolecules*, 2013, **46**, 2060–2066.
- A. J. Perkowski, W. You and D. A. Nicewicz, *J. Am. Chem. Soc.*, 2015, **137**, 7580–7583.
- K. A. Ogawa, A. E. Goetz and A. J. Boydston, *J. Am. Chem. Soc.*, 2015, **137**, 1400–1403.
- X. D. Liu, L. F. Zhang, Z. P. Cheng and X. L. Zhu, *Polym. Chem.*, 2016, **7**, 3576–3588.
- X. Liu, L. Zhang, Z. Cheng and X. Zhu, *Chem. Commun.*, 2016, **52**, 10850–10853.
- G. M. Miyake and J. C. Theriot, *Macromolecules*, 2014, **47**, 8255–8261.
- S. Shanmugam, J. Xu and C. Boyer, *Angew. Chem., Int. Ed.*, 2016, **55**, 1036–1040.
- C. Tian, P. Wang, Y. Ni, L. Zhang, Z. Cheng and X. Zhu, *Angew. Chem., Int. Ed.*, 2020, **59**, 3910–3916.
- L. Xiao, K. Sakakibara, Y. Tsujii and A. Goto, *Macromolecules*, 2017, **50**, 1882–1891.
- X. D. Liu, Q. H. Xu, L. F. Zhang, Z. P. Cheng and X. L. Zhu, *Polym. Chem.*, 2017, **8**, 2538–2551.
- Y. Zheng, S. Li, Z. Weng and C. Gao, *Chem. Soc. Rev.*, 2015, **44**, 4091–4130.

- 44 D. Wang, T. Zhao, X. Zhu, D. Yan and W. Wang, *Chem. Soc. Rev.*, 2015, **44**, 4023–4071.
- 45 H. J. Yang, Z. R. Wang, Y. L. Zheng, W. Y. Huang, X. Q. Xue and B. B. Jiang, *Polym. Chem.*, 2017, **8**, 2137–2144.
- 46 Y. Ge, C. Chen, X. M. Sim, J. Zheng and A. Goto, *Macromol. Rapid Commun.*, 2020, **41**, 1900623.
- 47 J. Zheng, C. G. Wang, Y. Yamaguchi, M. Miyamoto and A. Goto, *Angew. Chem., Int. Ed.*, 2018, **57**, 1552–1556.
- 48 C. Boyer, N. A. Corrigan, K. Jung, D. Nguyen, T. K. Nguyen, N. N. Adnan, S. Oliver, S. Shanmugam and J. Yeow, *Chem. Rev.*, 2016, **116**, 1803–1949.
- 49 J. Zheng, C. Chen and A. Goto, *Angew. Chem., Int. Ed.*, 2020, **59**, 1941–1949.
- 50 A. del Campo and E. Arzt, *Chem. Rev.*, 2008, **108**, 911–945.
- 51 J. O. Zoppe, N. C. Ataman, P. Mocny, J. Wang, J. Moraes and H. A. Klok, *Chem. Rev.*, 2017, **117**, 1105–1318.
- 52 T. Chen, I. Amin and R. Jordan, *Chem. Soc. Rev.*, 2012, **41**, 3280–3296.
- 53 A. Johnson, J. Madsen, P. Chapman, A. Alswieleh, O. Al-Jaf, P. Bao, C. R. Hurley, M. L. Cartron, S. D. Evans, J. K. Hobbs, C. N. Hunter, S. P. Armes and G. J. Leggett, *Chem. Sci.*, 2017, **8**, 4517–4526.
- 54 C. G. Wang, C. Chen, K. Sakakibara, Y. Tsujii and A. Goto, *Angew. Chem., Int. Ed.*, 2018, **57**, 13504–13508.
- 55 R. R. Bhat, M. R. Tomlinson, T. Wu and J. Genzer, *Surface-Grafted Polymer Gradients: Formation, Characterization, and Applications*, Springer Berlin Heidelberg, Berlin, Heidelberg, 2006.
- 56 X. Liu, C. G. Wang and A. Goto, *Angew. Chem., Int. Ed.*, 2019, **58**, 5598–5603.
- 57 C. G. Wang, A. Ming, L. Chong and A. Goto, *ACS Macro Lett.*, 2021, **10**, 584–590.
- 58 R. B. Grubbs, *Polym. Rev.*, 2011, **51**, 104–137.
- 59 Z. Wu, K. Jung and C. Boyer, *Angew. Chem., Int. Ed.*, 2020, **59**, 2013–2017.
- 60 D. A. Corbin and G. M. Miyake, *Chem. Rev.*, 2022, **122**, 1830–1874.